

Symmetry breaking with coupled Fano resonances

Björn Maes, Peter Bienstman, Roel Baets

Photonics Research Group, Ghent University,
St.-Pietersnieuwstraat 41, 9000 Ghent, Belgium
bjorn.maes@ugent.be

Abstract: We describe the effect of symmetry breaking in a system with two coupled Fano resonators. A general criterion is derived and optimal parameter regions for switching are identified. By extending the single resonator behavior we show that one achieves the effect at very low input powers.

© 2008 Optical Society of America

OCIS codes: (190.1450) Bistability; (230.4320) Nonlinear optical devices.

References and links

1. U. Fano, "Effects of configuration interaction on intensities and phase shifts," *Physical Review* **124**, 1866 (1961).
2. V. Lousse, and J.P. Vigneron, "Use of Fano resonances for bistable optical transfer through photonic crystal films," *Phys. Rev. E* **69**, 155106 (2004).
3. J.E. Heebner, R.W. Boyd, and Q-H. Park, "SCISSOR solitons and other novel propagation effects in microresonator-modified waveguides," *J. Opt. Soc. Am. B* **19**, 722–731 (2002).
4. B. Maes, P. Bienstman, and R. Baets, "Switching in coupled nonlinear photonic-crystal resonators," *J. Opt. Soc. Am. B* **22**, 1778–1784 (2005).
5. B. Maes, M. Soljačić, J.D. Joannopoulos, P. Bienstman, R. Baets, S-P. Gorza, and M. Haelterman, "Switching through symmetry breaking in coupled nonlinear micro-cavities," *Opt. Express* **14**, 10678–10683 (2006), <http://www.opticsinfobase.org/abstract.cfm?URI=oe-14-22-10678>.
6. P.E. Barclay, K. Srinivasan, and O. Painter, "Nonlinear response of silicon photonic crystal microresonators excited via an integrated waveguide and fiber taper," *Opt. Express* **13**, 801–820 (2005), <http://www.opticsinfobase.org/abstract.cfm?URI=oe-13-3-801>.
7. M. Notomi, A. Shinya, S. Mitsugi, G. Kira, E. Kuramochi, and T. Tanabe, "Optical bistable switching action of Si high-Q photonic-crystal nanocavities," *Opt. Express* **13**, 2678–2687 (2005), <http://www.opticsinfobase.org/abstract.cfm?URI=oe-13-7-2678>.
8. T. Uesugi, B-S. Song, T. Asano, and S. Noda, "Investigation of optical nonlinearities in an ultra-high-Q Si nanocavity in a two-dimensional photonic crystal slab," *Opt. Express* **14**, 377–386 (2006), <http://www.opticsinfobase.org/abstract.cfm?URI=oe-14-1-377>.
9. Y. Lu, J. Yao, X. Li, and P. Wang, "Tunable asymmetrical Fano resonance and bistability in a microcavity-resonator-coupled Mach-Zehnder interferometer," *Opt. Lett.* **30**, 3069–3071 (2005).
10. S. Fan, "Sharp asymmetric line shapes in side-coupled waveguide-cavity systems," *Appl. Phys. Lett.* **80**, 908–910 (2002).
11. P. Bienstman and R. Baets, "Optical modelling of photonic crystals and VCSELs using eigenmode expansion and perfectly matched layers," *Opt. Quantum Electron.* **33**, 327–341 (2001).
12. S. Fan, W. Suh, and J.D. Joannopoulos, "Temporal coupled-mode theory for the Fano resonance in optical resonators," *J. Opt. Soc. Am. A* **20**, 569–572 (2003).
13. M. Soljačić, M. Ibanescu, S.G. Johnson, Y. Fink, and J.D. Joannopoulos, "Optimal bistable switching in nonlinear photonic crystals," *Phys. Rev. E* **66**, 055601(R) (2002).

1. Introduction

The concept of a Fano resonance is very general [1]. It can arise in the context of an interaction between a localized or discrete resonance with a background or continuous channel. If the background is completely reflecting or transmitting, the effect of the resonance is a Lorentzian peak

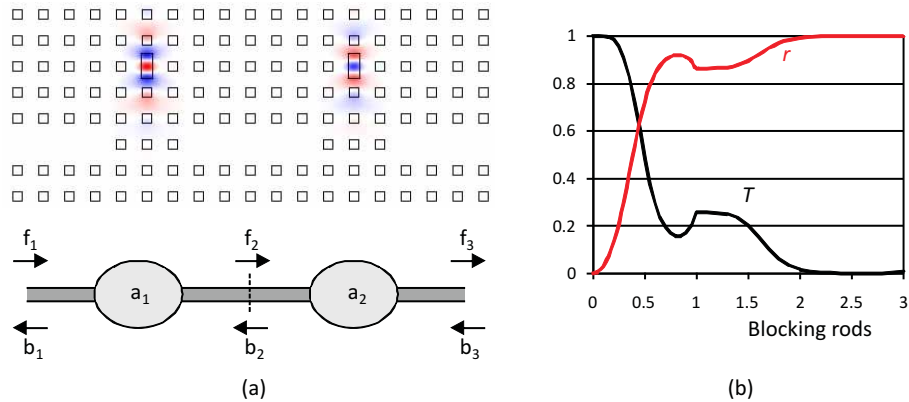


Fig. 1. (a) Schematic of the two-cavity device (bottom) and electric field plot of a device with three blocking rods per cavity (top). (b) Transmission T (black line) and reflection amplitude $r = \sqrt{1-T}$ (red line) versus number of blocking rods in the PhC waveguide at wavelength $a/0.367$.

or dip. If the background is partially reflecting, the more general transition with two extrema is obtained (see e.g. Fig. 2(b)).

In the optical domain, these resonances are commonplace, as beams in free-space or waveguides couple with cavities. The single peak Lorentzian case is most studied, both in the linear and nonlinear domain for filtering and switching purposes, respectively. It was realized that the more general resonances lead to different switching possibilities in one-cavity devices [2]. Coupling of multiple Lorentz-type cavities also proved to be a promising field for nonlinear functionality [3, 4].

Recently we proposed a switching device that employs a symmetry-breaking bifurcation [5]. This breaking occurs because of the feedback between two nonlinear cavities. In the linear regime the structure is left-right symmetric, see Fig. 1(a), and we excite the system with equal powers from both sides. Linearly this results in equal output powers to the left and to the right. At higher powers, however, an instability can appear, and the structure becomes asymmetric: one cavity will be more excited than the other, resulting in index differences through the Kerr effect, leading to feedback away from the symmetric solution. In such a structure the two *equal* input powers result in two *different* output powers, as the fields of both inputs interfere constructively on one side and destructively on the other.

Because of the symmetry of the linear system, there are always two equivalent asymmetric states: one where the left output power is larger than the right output power, and the mirrored state, where the right output is larger than the left output. By increasing or decreasing one of the inputs, it is possible to switch between these two states. Thus, this scheme provides the option of switching with positive pulses, which is not obvious in single-cavity devices. In addition, the dynamical interaction between two cavities can be tuned judiciously, so interesting regimes are available, as we show later.

In this paper we broaden the study of the symmetry-breaking device by considering the entire class of Fano resonances, instead of the single Lorentzian case. A general analytical criterion for the existence of the effect is derived. The generalization leads to additional optimization possibilities, and we show e.g. that low-power effects are feasible.

We mainly consider the context of photonic crystal (PhC) waveguides and cavities. These structures offer the possibility for highly compact, efficient devices. Single cavity switching has already been demonstrated experimentally [6, 7, 8]. The results are more general however,

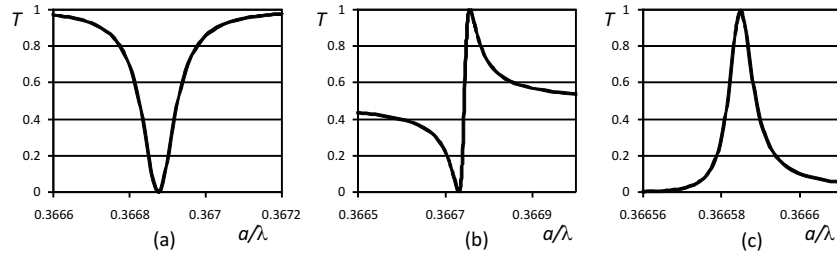


Fig. 2. Transmission T in three different cavity structures: (a) no blocking rods ($T_{\text{background}} \approx 1$); (b) one blocking rod with side $0.2a$ ($T_{\text{background}} \approx 0.5$); (c) three blocking rods ($T_{\text{background}} \approx 0$).

as the generic coupled-mode theory (CMT) is employed. Indeed, Fano resonances have also been demonstrated in other contexts such as ring resonators [9] and PhC films [2].

The paper is structured as follows. First we shortly review the characteristic Fano shapes in a PhC system. Then we use CMT to derive a general criterion for the existence of symmetry breaking solutions. In the next section the extra degree of freedom is employed to optimize some switching features.

2. Fano resonances

A PhC system with a single-cavity coupled to a waveguide (one side of the field plot in Fig. 1(a)) can show the whole range of Fano resonances [10]. The shape of the transmission curve in this configuration is determined by the waveguide properties. This direct channel is adjustable by adding or removing rods in the waveguide. Fine-tuning is possible by changing rod radii. The result of such a modeling exercise is shown in Fig 1(b). This presents the transmission T through the waveguide, without the cavity, in function of the ‘number’ of blocking rods. If this number is between 0 and 1 we increase the radius of a single blocking rod. In contrast, between 1 and 3, we increase the radii of two rods adjacent to a rod which is already the same size as the lattice rods. The discontinuous connection follows from this approach. Clearly, the system is tunable between complete and zero transmission.

If a cavity is added next to the waveguide, the transmission has specific shapes around the resonance frequency. If the channel is obstructed by a number of rods, the waveguide transmission is almost zero. However, on resonance all light is coupled via the cavity to the output port, and a Lorentzian transmission spectrum is obtained, see Fig. 2(c). In contrast, if the channel is unobstructed the transmission is zero on resonance, so one gets a Lorentzian dip, see Fig. 2(a). In between, a range of background transmission between zero and one is possible. In that case the transmission shows two extrema, with a zero and complete transmission frequency next to each other, see Fig. 2(b).

The modeled two-dimensional PhC system is embedded in a square lattice with period a of square rods with side $0.4a$. The rods have index 3.5 in an air background. The waveguide is formed by removing a row of rods. The cavity is created by a rectangular defect rod with dimensions $a \times 0.48a$. Calculations are performed with the mode expansion method [11].

3. General criterion

The coupled-mode equations for this structure are [12, 4]:

$$\frac{da_j}{dt} = \left[i(\omega_0 + \delta\omega_j) - \frac{1}{\tau} \right] a_j + df_j + db_{j+1}, \quad (1)$$

$$\begin{bmatrix} b_j \\ f_{j+1} \end{bmatrix} = \exp(i\phi) \begin{bmatrix} r & it \\ it & r \end{bmatrix} \cdot \begin{bmatrix} f_j \\ b_{j+1} \end{bmatrix} + da_j \begin{bmatrix} 1 \\ 1 \end{bmatrix}, \quad (2)$$

for $j = 1, 2$. The complex a_j are cavity mode amplitudes, so $|a_j|^2$ is the energy in the mode. The f_j and b_j are waveguide mode amplitudes, thus $|f_j|^2$ (resp. $|b_j|^2$) represents the power flowing in the (single-mode) waveguide in the forward (resp. backward) direction, see Fig. 1(a). Both cavities have the same resonance frequency ω_0 and lifetime τ . The nonlinear frequency shift is $\delta\omega_j = -|a_j|^2/(P_0\tau^2)$, with P_0 the ‘characteristic nonlinear power’ of the cavities [13], which we discuss below. The coupling parameter in this system is $d = i\exp(i(\phi + \beta)/2)/\sqrt{\tau}$, where $\beta = \text{atan}(t/r)$. The real constants ϕ , t and r determine the direct channel properties. The reflection and transmission are coupled by $r^2 + t^2 = 1$.

The input power on the left side is $P_{in}^L \equiv |f_1|^2$, on the right side we have as input $P_{in}^R \equiv |b_3|^2$. In this paper the input powers are equal, so we note $P_{in} \equiv P_{in}^L = P_{in}^R$. The output powers are $P_{out}^L \equiv |b_1|^2$ and $P_{out}^R \equiv |f_3|^2$ on the left and right side, respectively. For symmetry-breaking states one has $P_{out}^L \neq P_{out}^R$.

The parameter ϕ plays a central role in the dynamical behavior of the system, and thus in our analysis. It depends on the precise reflection and transmission effects because of the blocking rods (if any) next to the resonator. But, more importantly, it is fully controllable by adjusting the length of the waveguide in between the resonators. In PhC systems this length is adjusted by changing the number of periods. However, this is not limiting: The phase ϕ is invariant with period 2π , and the propagation factor k_z of PhC waveguides is not difficult to tune. If there are no blocking rods, we have $\phi = -mk_z a - \pi/2$, with m the number of periods in one half of the device.

The parameter P_0 allows to evaluate the power levels for the operation of nonlinear devices. In [13] it is defined for a single cavity as $P_0 = c/(\kappa Q^2 \omega_0 n_2)$, with c the speed of light, $Q = \omega_0 \tau/2$ the quality factor, and n_2 the nonlinear Kerr material coefficient. κ is a dimensionless nonlinear strength parameter, which is proportional to the overlap of the resonator mode with the nonlinear material region [13]. We normalize all our powers with respect to P_0 . Indeed, this P_0 indicates the power level at which nonlinear effects appear in single cavity nonlinear devices. E.g. in a structure with a single cavity that is blocked ($r=1$), one can show that the minimum input power for the standard bistability effect is $\sqrt{3}P_0$ [13]. Further on we will obtain that significantly lower switching powers are achievable in the two-cavity devices.

In the following we obtain a criterion for this general system. It determines for which frequencies one expects asymmetric states. The analysis is an extension of the method in [5]. We work in the frequency domain so d/dt becomes $i\omega$. Eliminating f_2 and b_2 we obtain:

$$\left[i(\omega_0 - \omega + \delta\omega_1) - \frac{1}{\tau} \right] a_1 + \kappa d(c_1 a_1 + a_2) = -(d + \kappa c_1 c_2) f_1 - \kappa c_2 b_3, \quad (3)$$

$$\left[i(\omega_0 - \omega + \delta\omega_2) - \frac{1}{\tau} \right] a_2 + \kappa d(c_1 a_2 + a_1) = -(d + \kappa c_1 c_2) b_3 - \kappa c_2 f_1, \quad (4)$$

with $c_1 = r\exp(i\phi)$, $c_2 = it\exp(i\phi)$ and $\kappa = d/(1 - c_1^2)$. We equate the left sides of Eqs. 3 and 4, as we assume equal input power and phase from both sides, so $f_1 = b_3$. We take the modulus squared, and after factoring we get:

$$(A - B) [(A^2 + AB + B^2) + 2(\Delta + \Gamma_1)(A + B) + \Delta^2 + 2\Delta\Gamma_1 + \Gamma_2] = 0, \quad (5)$$

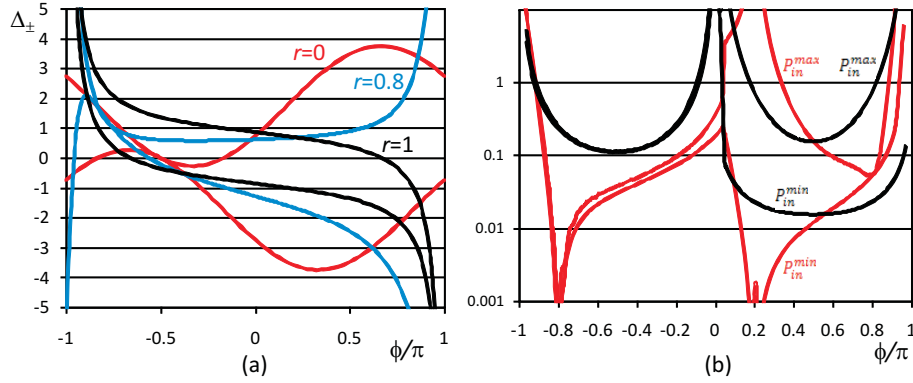


Fig. 3. (a) Critical detunings Δ_{\pm} for $r = 1$ (black lines), $r = 0.8$ (blue lines) and $r = 0$ (red lines), respectively. The largest value is Δ_+ , the smallest corresponds to Δ_- . (b) Minimum input power P_{in}^{min} and corresponding P_{in}^{max} versus ϕ for $r = 1.0$ (black lines) and $r = 0.8$ (red lines), respectively. For these results P_{in}^{min} was minimized. All powers in units of P_0 .

with dimensionless cavity energies $A = \alpha|a_1|^2$ and $B = \alpha|a_2|^2$, where $\alpha = -1/(P_0\tau)$. In addition, the detuning is $\Delta = \tau(\omega_0 - \omega)$ and

$$\Gamma_1 = (rt + r\sin\phi + t\cos\phi)/(1 + 2r\cos\phi + r^2), \quad (6)$$

$$\Gamma_2 = (1 + 2t\sin\phi + t^2)/(1 + 2r\cos\phi + r^2). \quad (7)$$

Starting with the discriminant from Eq. 5 one obtains the critical detunings

$$\Delta_{\pm} = -\Gamma_1 \pm \sqrt{3(\Gamma_2 - \Gamma_1^2)}. \quad (8)$$

For positive nonlinearity ($\alpha < 0$) one needs $A < 0$, which means that the asymmetric solution ($A \neq B$) exists if $\Delta > \Delta_+$. For negative nonlinearity one obtains that $\Delta < \Delta_-$. For $r = 1$ Eq. 8 reduces to the previous criterion [5].

The critical detunings for different structures are shown in Fig. 3(a). It appears that the asymmetric solutions exist for all r -values, except for some phases where the critical detuning becomes infinite. However, the usefulness of the nonlinear switching curves depends on the application, the power levels etc. Therefore, in the next section an analysis is performed to identify practical parameter regions.

4. Optimization

In this section we provide insight into optimal parameter choices. In addition we show how some features of the nonlinear switching behavior are correlated with the linear properties. We note that this system has many parameters with a profound influence on the characteristics. Furthermore, the figure of merit that one may define depends on the envisaged application.

In this paper our first focus is on the minimum input power P_{in}^{min} that is needed to observe symmetry breaking states. Above this power, the symmetric solution becomes unstable. Subsequently, we examine the maximum input power P_{in}^{max} at which point the nonlinear asymmetric 'eye' closes (see e.g. Fig.4(a), also discussed below). Above this input power, the symmetric solution is stable again. Thus, asymmetric states are observable in the range of input powers between P_{in}^{min} and P_{in}^{max} . If this P_{in}^{max} is too large, it will be difficult to switch by using positive pulses. On the other hand, if P_{in}^{max} is too close to P_{in}^{min} the range of symmetry breaking input powers is too narrow for comfortable switching.

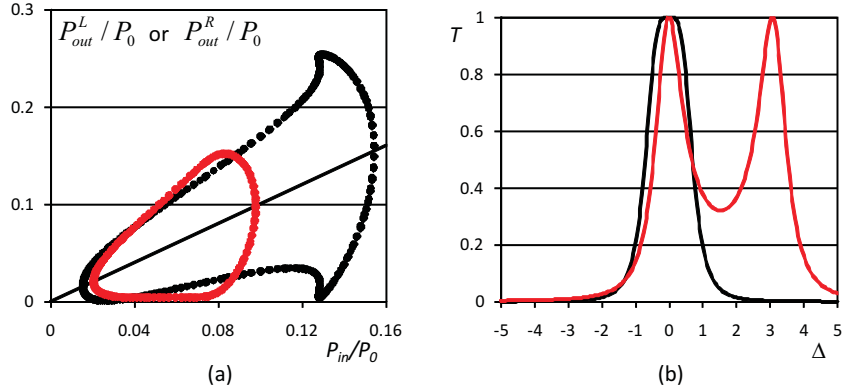


Fig. 4. (a) Asymmetric states for $r = 1$, $\phi = 0.5\pi$ with $\Delta = 1.02$ (black dots) and $\Delta = 0.62$ (red dots), respectively. The symmetric states are shown with a line. (b) Linear transmission T versus detuning Δ with $r = 1$ for $\phi = 0.5\pi$ ($\phi = 0.1\pi$) in black (red), respectively.

A next characteristic to examine is the contrast between the output powers in the asymmetric state. Ideally this contrast should be large over a wide range of input powers, which means that the output power to one side is much larger than the output power to the other side.

To examine P_{in}^{min} we perform a parameter sweep: For a fixed ϕ and r value we iterate over a range of detunings Δ (where, according to the criterion, symmetry breaking appears). Every ϕ and r combination corresponds to one Δ with the smallest input power for symmetry breaking P_{in}^{min} .

4.1. Perfect reflection

First, we examine the perfect reflection case, or $r = 1$. Figure 3(b)(black lines) shows the sweep results in this case; it plots the minimum P_{in}^{min} versus ϕ . It is evident that $\phi = 0.5\pi$ is the most interesting point, as it has the lowest P_{in}^{min} . We also plot the corresponding P_{in}^{max} in Fig. 3(b). Remark that P_{in}^{min} is quite insensitive to the exact phase, whereas P_{in}^{max} shows a stronger variation.

For ϕ in $[-\pi, 0]$ we see that $P_{in}^{min} \approx P_{in}^{max}$, so that the range of asymmetry is too small. On the contrary, at $\phi = 0.5\pi$ there is a comfortable order of magnitude difference between P_{in}^{min} and P_{in}^{max} . This operational point is therefore very advantageous. Two nonlinear switching curves for $r = 1$ are shown in Fig. 4(a). These curves show P_{out}^L and P_{out}^R versus P_{in} . The straight line through the origin presents the symmetric solutions, where $P_{out}^L = P_{out}^R$. The curves formed by the dots are the asymmetric solutions, meaning $P_{out}^L \neq P_{out}^R$. Note the mirrored nonlinear solutions: if there is a state with $P_{out}^L > P_{out}^R$, there is an equivalent one with $P_{out}^L < P_{out}^R$. The linear solutions are unstable when the symmetric straight line lies inside the asymmetric eye, as linear stability analysis shows, indicating the experimental legitimacy of the asymmetric solutions. The nonlinear curves can have interesting shapes, see the black curve in Fig. 4(a). It was determined that the parts with different curvature around $P_{in}/P_0 = 0.125$ are unstable, leading to four stable asymmetric states [5].

The system with the smallest P_{in}^{min} has $\Delta = 1.02$ and is shown in black. If we decrease the detuning, we also find we can obtain flat, high-contrast output powers (Fig. 4(a)(red dots)). The latter devices provide useful contrast for digital logic applications. In addition, the necessary P_{in}^{min} is still adequate.

We find an indicative link with the linear transmission properties, in the case of a single input. Some transmission curves are shown in Fig. 4(b). We remark that we work in the case of $r = 1$,

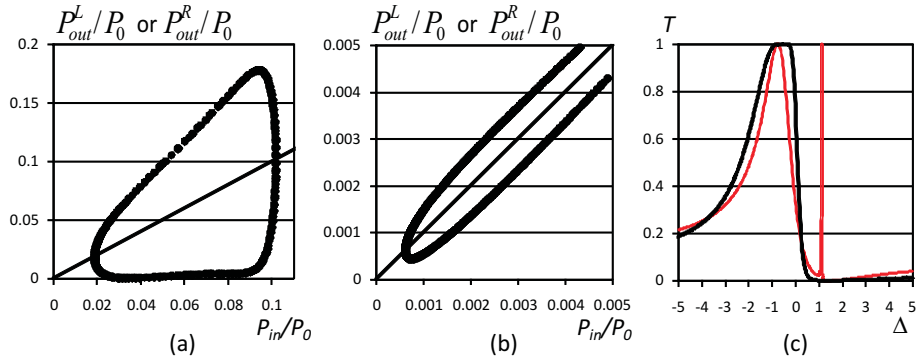


Fig. 5. Asymmetric states for (a) $r = 0.8$, $\phi = 0.6\pi$, $\Delta = 1.25$ and (b) $r = 0.8$, $\phi = 0.23\pi$, $\Delta = 2.1$. The symmetric states are shown with a line. (c) Linear transmission T versus detuning Δ with $r = 0.8$ for $\phi = 0.6\pi$ ($\phi = 0.23\pi$) in black (red), respectively.

so the background (without cavities) is perfectly reflecting. However, in the presence of cavities the light can tunnel through the resonators and pass the barriers, which leads to frequencies with perfect transmission. Note that the transmission curves for ϕ and $\phi + \pi$ look the same. However, the phases of the underlying amplitudes are different. Therefore, the nonlinear dynamics of ϕ and $\phi + \pi$ are dissimilar, which is already clear from Fig. 3(b) by comparing the ϕ -ranges $[-\pi, 0]$ and $[0, \pi]$. However, there are similar trends, see e.g. Fig. 3(b): both have extrema at $\phi = -0.5\pi$ and $\phi = 0.5\pi$.

It is known that the linear transmission of such two-cavity systems shows two peaks whose relative positions depend on ϕ [4], see Fig. 4(b). The values $\phi = \pm 0.5\pi$ are special cases, because then the two peaks coalesce into one broader peak, see Fig. 4(b)(black curve). This broader peak has steeper sides, which is often advantageous for nonlinear effects, and thus here too for low power symmetry breaking. Indeed, from the definition of the characteristic power we note that $P_0 \sim 1/Q^2$. So, in the single cavity case, there is a direct link between steepness of the linear transmission curve (Q) and nonlinear switching power levels (P_0). Although, we do not define Q and P_0 for two-cavity devices, it is clear that a steep transmission curve correlates with a low switching power. An interpretation of this is that for nonlinear effects the linear curve shifts towards the operating frequency, and large slopes result in low powers to instigate this shift.

4.2. Imperfect reflection

Here we discuss the changes in the previous analysis if $r \neq 1$. Figure 3(b)(red lines) shows P_{in}^{min} and P_{in}^{max} for $r = 0.8$, which means that 64% ($= r^2$) of the power is reflected. This has to be compared with the curves for $r = 1$ (black lines in Fig. 3(b)). In the range $[-\pi, 0]$ we see again that P_{in}^{min} and P_{in}^{max} follow each other closely, which makes observation of asymmetry difficult.

We note that in $[0.5\pi, \pi]$ the minimum input power P_{in}^{min} is larger for $r = 0.8$ than for $r = 1$. In addition, P_{in}^{max} becomes smaller in this range. In the range $[0.5\pi, 0.75\pi]$ it is common to see acceptable nonlinear switching curves, see Fig. 5(a). P_{in}^{min} is not as small as for $r = 1$, but P_{in}^{max} can be tuned favorably. The linear transmission curve for this situation, see Fig. 5(c)(black curve), shows that the peaks coalesce into one broader peak, similar to the previous total reflection case.

An important difference between the perfect and imperfect reflection cases is the appearance of ϕ values with extremely low P_{in}^{min} . For $r = 0.8$ this is the case around $\phi = -0.8\pi$ and $\phi = 0.2\pi$. However, in $[0, 0.5\pi]$ the value of P_{in}^{max} becomes high, so positive pulse switching is

unlikely (one needs to go beyond P_{in}^{max}). With ϕ around 0.23π e.g. it is possible to have low power asymmetric states, see Fig. 5(b). The P_{in}^{min} drops by an order of magnitude, below $10^{-3} \times P_0$. A disadvantage in these cases is that the contrast between the output powers is often limited.

The origin of the dips in P_{in}^{min} is apparent from the linear transmission curves, see Fig. 5(c)(red curve). By coupling two cavities with $r \neq 1$ one can obtain vanishingly narrow transmission peaks, which evidently have their impact on nonlinear switching properties [4]. As noted in the end of the previous section, such a very steep slope corresponds to a very low switching power. Indeed, in Fig. 5(b), the bifurcation power is three orders of magnitude lower than P_0 . Thus, the extremely narrow peaks are easily shifted by nonlinearity. This interference effect is not available in the perfectly reflecting case.

5. Conclusions

We extended the description of symmetry breaking in two coupled nonlinear cavities. We describe the appearance of the effect for the larger class of Fano resonances. As was the case with coupled Lorentzian resonators an elegant analytical description is employed and a criterion for the emergence of asymmetric states is derived. In addition, we optimize the switching scheme: we determine the parameter regimes where low input powers or high contrast output powers appear. This indicates which structures would be most promising for experimental verification. The perfectly reflecting structure with an inter-cavity phase around $\phi = \pi/2$ is appropriate for switching operations with positive pulses and has a good contrast. Extremely low bifurcation powers, much lower than for single cavity devices, are obtained in a structure with partial reflection. This corresponds to the appearance of very narrow transmission peaks in the linear spectrum.

Acknowledgments

BM acknowledges a postdoctoral fellowship from the Funds for Scientific Research - Flanders (FWO-Vlaanderen). We acknowledge the Belgian IUAP project Photonics@be.